

by Keith H. Coats, Intercomp Resource Development and Engineering, Inc.

© Copyright 1979, American Institute of Mining, Metallurgical, and Petroleum Engineers, Inc.

This paper was presented at the 54th Annual Fall Technical Conference and Exhibition of the Society of Petroleum Engineers of AIME, held in Las Vegas, Nevada, September 23-26, 1976. The material is subject to correction by the author. Permission to copy is restricted to an abstract of not more than 300 words. Write 6200 N. Central Expy., Dallas, Texas 75208.

ABSTRACT

This paper describes an implicit, three-dimensional formulation for simulating compositional-type reservoir problems. The model treats three-phase flow in Cartesian (x-y-z) or cylindrical (r-θ-z) geometries. Applicability ranges from depletion or cycling of volatile oil and gas condensate reservoir to miscible flooding operations involving either outright or multiple-contact-miscibility.

The formulation utilizes an equation of state for phase equilibrium and property calculations. The equation of state provides consistency and smoothness as gas and oil phase compositions and properties converge near a critical point. This avoids computational problems near a critical point associated with use of different correlations for K-values as opposed to phase densities.

Computational testing with example multiple-contact miscibility (MCM) problems indicates stable convergence of this formulation as phase properties converge at a critical point. Results for these MCM problems show significant numerical dispersion, primarily affecting the calculated velocity of the miscible front advance. Our continuing effort is directed toward reduction of this numerical dispersion and comparison of model results with laboratory experiments for both multiple-contact and outright miscibility cases.

We feel that the implicit nature of the model enhances efficiency as well as reliability for most compositional type problems. However, while we report detailed problem results and associated computing times, we lack similar reported times to compare the overall efficiency of an implicit compositional formulation with that of a semi-implicit formulation.

INTRODUCTION

Many papers have treated increasingly sophisticated or efficient methods for numerical modeling of black oil reservoir performance. The latter type of reservoir allows an assumption that reservoir gas and oil have

different but fixed compositions with the solubility of gas in oil being dependent upon pressure alone.

A smaller number of papers have presented numerical models for simulating isothermal "compositional" reservoirs where oil and gas equilibrium compositions vary considerably with spatial position and time. With some simplification, the reservoir problems requiring compositional treatment can be divided into two types. The first type is depletion and/or cycling of volatile oil and gas condensate reservoirs. The second type is miscible flooding with multiple-contact-miscibility (MCM) generated in-situ.

A distinction between these types is that the first usually involves phase compositions removed from the critical point while the second type generally requires calculation of phase compositions and properties converging at the critical point. A compositional model is or should be capable of treating the additional problem of outright miscibility where the original oil and injected fluid are miscible upon first contact.

A difficulty in modeling the MCM process is achievement of consistent, stable convergence of gas and oil phase compositions, densities and viscosities as the critical point is approached. A number of studies have reported models which utilize different correlations for equilibrium K-values as opposed to phase densities¹⁻⁵. Use of an equation of state offers the advantage of a single, consistent source of calculated K-values, phase densities and their densities near a critical point.

The purpose of this work was to develop, and test with sample problems, a multidimensional, compositional model using an equation of state. While this objective includes applicability to depletion, cycling and outright miscible flooding operations, our emphasis in this work was placed on simulation of the MCM process.

References and illustrations at end of paper.

Van-Quy et al⁶ described a one-dimensional, two-phase (gas-oil), compositional model neglecting gravity and capillary forces. They utilized a 3-component correlation guaranteeing consistency of phase compositions and properties at the critical point and presented detailed calculated and some experimental one-dimensional results for vaporizing and condensing (MCM) gas injection cases. Corteville et al⁷ used the same model and presented additional comparisons between linear calculated and experimental results.

Metcalf et al⁸ and Fussell et al⁹ published two studies using a cell-to-cell flash calculation model¹⁰ to simulate the MCM or vaporizing gas injection process. Fussell and Yanosik¹¹ described iterative methods for phase equilibria calculations using a modified Redlich-Kwong equation of state. Fussell and Fussell¹² utilized the latter work in developing a formulation for a multidimensional compositional model. They presented an example calculation for an immiscible gas injection case.

This paper describes an equation of state, implicit compositional model formulation for three-dimensional, three-phase flow under viscous, gravity and capillary forces. Test applications to one- and two-dimensional MCM type problems are described. This paper reports the capability of this formulation in computationally coping with the convergence problems encountered near critical points in the MCM process. Our continuing effort is directed toward comparisons with published experimental data, for both MCM and outright miscibility processes, and further examination and reduction of numerical dispersion error.

GENERAL DESCRIPTION OF THE MODEL

The model formulation treats one- two- or three-dimensional flow of water, oil and gas in formations of heterogeneous permeability and porosity with Cartesian (x-y-z) or cylindrical (r-θ-z) geometries. The fluid flow is simulated using Darcy's law incorporating gravity and viscous and capillary forces. Relative permeability and capillary pressure are dependent upon saturations and interfacial tension.

The model applies to depletion of volatile oil or gas condensate reservoirs and cycling of the latter. However, the primary objective of this work was development and testing of a model capable of simulating vaporizing gas injection and miscible flooding operations. In the test applications described below we emphasize the multiple-contact-miscibility process.

The model consists of mass balances for water and N_c hydrocarbon components and associated constraint equations. Oil and gas phase densities and fugacities or K-values are calculated from a modified Redlich-Kwong equation of state^{13,14}. Oil and gas phase viscosities are calculated from the Lohrenz, Bray and Clark method¹⁵ and converge to a common value as the phase compositions converge near a critical point. Interfacial tension is calculated from the Macleod-Sugden correlation¹⁶.

The formulation is implicit and requires simultaneous solution of a set of $N_c + 1$ finite difference equations throughout the grid representing the reservoir. This implicit formulation requires more arithmetic (computing time) per grid block per time step than an IMPES (implicit pressure-explicit saturation) type of model. However, the latter treats transmissibilities explicitly in saturation and composition variables and accordingly tends to require smaller and more time steps than an implicit model. We have not yet compared overall efficiencies of the two types of models.

Formulation assumptions are instantaneous equilibrium between gas and oil phases in any grid block and mutual insolubility of water and hydrocarbon components. There are no assumptions or limits on the number of hydrocarbon components, other than computer storage and computing time requirements. Diffusion is neglected.

Material balance error for each component is printed after calculation as (initial-in-place + cumulative injection-cumulative production-(actual-in-place))/Max(cumulative injection, cumulative production), where all quantities are in moles. This fractional error is consistently less than ± .0001.

PVT treatment of fluid and rock properties is described in the Appendix.

MATHEMATICAL MODEL DESCRIPTION

The model consists of N equations written in finite difference form for each grid block, where N is $2N_c + 4$. The N_c component mass balances are

$$\frac{V}{\Delta t} \bar{\delta} [\phi(\rho_o S_o x_i + \rho_g S_g y_i)] = \Delta(T\rho_o x_i \frac{k_{ro}}{\mu_o} (\Delta p - \Delta p_{cgo} - \gamma_o \Delta Z)) + \Delta(T\rho_g y_i \frac{k_{rg}}{\mu_g} (\Delta p - \gamma_g \Delta Z)) - q_i \quad i = 1, 2, \dots, N_c \quad (1)$$

The water mass balance is

$$\frac{V}{\Delta t} \bar{\delta} (\phi \rho_w S_w) = \Delta(T\rho_w \frac{k_{rw}}{\mu_w} (\Delta p - \Delta p_{cgo} - \Delta p_{cwo} - \gamma_w \Delta Z)) - q_w \quad (2)$$

The N_c fugacity constraints

$$f_i^L - f_i^V = 0 \quad i = 1, 2, \dots, N_c \quad (3)$$

express the requirement that liquid and vapor phase fugacities must be equal for each component. The 2 mol fraction constraints

$$\sum_{i=1}^{N_c} x_i = 1.0 \quad (4a)$$

$$\sum_{i=1}^{N_c} y_i = 1.0 \quad (4b)$$

and the saturation constraint

$$S_o + S_g + S_w = 1.0 \quad (5)$$

complete the set of N model equations.

The N unknowns corresponding to these equations are

$$x_1, x_2, \dots, x_{N_c}, y_1, y_2, \dots, y_{N_c}, p, S_o, S_g, S_w \quad (6)$$

and these unknowns will be referred to hereafter as $\{P_i\}$ where $P_1 = x_1, P_2 = x_2, \dots, P_N = S_w$, in the order listed in (6).

In order to solve these N equations, all terms must be expanded into linear combinations of the selected dependent variables or unknowns. In the implicit formulation described here the N unknowns at each time step are $\{\delta P_i\}$ for each grid block.

Our notation is, for any quantity or product of terms X,

$$\begin{aligned} \bar{\delta}X &= X_{n+1} - X_n \\ \delta X &= X^{l+1} - X^l \end{aligned} \quad (7)$$

where subscript n denotes time level, X_n is known because all variables are known at the old time level and superscript l is iterate number. Thus $\bar{\delta}X$ is the change in X over the time step while δX is the change in X over one iteration.

The time difference is approximated by

$$\bar{\delta}X \approx \delta X + X^l - X_n \quad (8)$$

which becomes an exact equality as $X^{l+1} \rightarrow X_{n+1}$. Implicit treatment of interblock flow and well terms and quantities in the constraints simply consists of expressing the terms at time level n + 1:

$$X_{n+1} \approx X^{l+1} = X^l + \delta X \quad (9)$$

Finally, the term δX is expanded as a linear combination of the N dependent variables or unknowns $\{P_i\}$ as

$$\delta X \approx \sum_{j=1}^N \left(\frac{\partial X}{\partial P_j} \right)^l \delta P_j \quad (10)$$

where the derivatives are evaluated at the latest iterate values of $\{P_i\}$. Derivatives of products of terms are obtained by the normal chain rule,

$$\frac{\partial(abc)}{\partial P} = (bc) \frac{\partial a}{\partial P} + ac \frac{\partial b}{\partial P} + ab \frac{\partial c}{\partial P} \quad (11)$$

Expansion of Accumulation Terms

The time-difference or accumulation terms on the left-hand side of the mass balances are expanded as illustrated here for component 1,

$$\begin{aligned} \bar{\delta} [\phi(\rho_o S_o x_1 + \rho_g S_g y_1)] &= [\phi(\rho_o S_o x_1 + \rho_g S_g y_1)]^k - \\ &[\phi(\rho_o S_o x_1 + \rho_g S_g y_1)]_n + \sum_{j=1}^N \frac{\partial}{\partial P_j} \\ &[\phi(\rho_o S_o x_1 + \rho_g S_g y_1)]^l \delta P_j \end{aligned} \quad (12)$$

where for illustration,

$$\frac{\partial}{\partial x_j} [\phi(\rho_o S_o x_1 + \rho_g S_g y_1)] = \phi S_o (\rho_o \delta_{ij} + x_1 \frac{\partial \rho_o}{\partial x_j}) \quad (13)$$

$$\begin{aligned} \frac{\partial}{\partial p} [\phi(\rho_o S_o x_1 + \rho_g S_g y_1)] &= \phi (S_o x_1 \frac{\partial \rho_o}{\partial p} + S_g y_1 \frac{\partial \rho_g}{\partial p}) \\ &+ (\rho_o S_o x_1 + \rho_g S_g y_1) \frac{\partial \phi}{\partial p} \end{aligned} \quad (14)$$

and δ_{ij} is the Dirac delta function.

Expansion of Interblock Flow Terms

The interblock flow terms on the right sides of the mass balances are evaluated implicitly as illustrated for x-direction flow of component 1 in the gas phase between adjacent grid blocks 1 and 2:

$$\begin{aligned} \Delta(T_x \rho_g y_1 \frac{k_{rg}}{\mu_g} (\Delta p - \gamma_g \Delta Z)) &= T_x (\rho_g y_1 \frac{k_{rg}}{\mu_g} (\Delta p - \gamma_g \Delta Z))^l \\ &+ T_x \sum_{j=1}^N \frac{\partial}{\partial P_j} (\rho_g y_1 \frac{k_{rg}}{\mu_g} (\Delta p - \gamma_g \Delta Z))^l \delta P_j \end{aligned} \quad (15)$$

k_{rg}, μ_g, ρ_g and y_1 are evaluated at the upstream block and

$$\gamma_g = \omega \gamma_{g1} + (1 - \omega) \gamma_{g2} \quad (16)$$

where

$$\omega = V_1 \phi_1 / (V_1 \phi_1 + V_2 \phi_2) \quad (17)$$

if S_g is nonzero in both grid blocks. If S_g is nonzero only in the upstream block then γ_g is evaluated upstream.

Treatment of Well Terms

We illustrate the semi-implicit treatment of well terms for production of component 1 from a well on deliverability completed in layers $k = 1, 2$ and 3 . The rate of production from layer k is

$$q_{i,k} = PI_k \left\{ \left[\rho_o \frac{k_{ro}}{\mu_o} x_i + \rho_g \frac{k_{rg}}{\mu_g} y_i \right]_k (P_k - P_{wbk}) \right\}^{\lambda} + \sum_{j=1}^N \frac{\partial}{\partial P_j} \left[\left(\rho_o \frac{k_{ro}}{\mu_o} x_i + \rho_g \frac{k_{rg}}{\mu_g} y_i \right)_k (P_k - P_{wbk}) \right]^{\lambda} \delta P_j \quad (18)$$

The wellbore pressure gradient is calculated using an explicit wellbore gradient as

$$P_{wbk} = P_{wb,k-1} + \bar{\gamma} (Z_k - Z_{k-1}) \quad (19)$$

where P_{wb1} = the specified bottom-hole flowing pressure, Z_k is subsea depth opposite the center of layer k and

$$\bar{\gamma} = \left\{ \sum_{k=1}^3 PI_k (\lambda_o \gamma_o + \lambda_g \gamma_g + \lambda_w \gamma_w) P_k / \sum_{k=1}^3 PI_k (\lambda_o + \lambda_g + \lambda_w) P_k \right\}_n \quad (20)$$

Expansion of Constraint Equations

The fugacity constraints, Equation (3), are approximated implicitly (at time level $n+1$) using

$$f_{i,n+1} \approx f_i^L + \sum_{j=1}^{2N_c+1} \left(\frac{\partial f_i}{\partial P_j} \right)^L \delta P_j \quad (21)$$

where f_i is dependent only upon mol fractions and pressure and is independent of saturations. Use of (21) in Equation (3) gives

$$\sum_{j=1}^{2N_c+1} \frac{\partial}{\partial P_j} (f_i^L - f_i^V)^L \delta P_j = (f_i^V - f_i^L)^L \quad (22)$$

$$i = 1, 2, \dots, N_c$$

Of course, f_i^L is dependent only upon $\{x_i\}$ and p and f_i^V is dependent only upon $\{y_i\}$ and p . The constraints are expressed implicitly as

$$\sum_{i=1}^{N_c} \delta x_i = 1.0 - \sum_{i=1}^{N_c} x_i^L \quad (23a)$$

$$\sum_{i=1}^{N_c} \delta y_i = 1.0 - \sum_{i=1}^{N_c} y_i^L \quad (23b)$$

$$\delta S_o + \delta S_g + \delta S_w = 1.0 - (S_o + S_g + S_w)^L \quad (24)$$

Consolidation of N Model Equations

When written for a given grid block, the first $N_c + 1$ of the N model Equations (1) - (5) involve unknowns $\{\delta P_j\}$ for that grid block and in addition involve the unknowns $\{\delta P_j\}$ of each neighboring block. This appearance of adjacent block unknowns is a result of the interblock flow terms present in the mass balances. We refer to these $N_c + 1$ mass balances as the "primary" equations. The remaining $N_c + 3$ (constraint) Equations (3) - (5) involve only the unknowns $\{\delta P_j\}$ of the given grid block. Therefore they can be used to eliminate $N_c + 3$ unknowns from the primary equations, resulting in a set of $N_c + 1$ primary equations in $N_c + 1$ unknowns.

The expanded constraint Equations (22) and (23) are $N_c + 2$ equations in $2N_c + 1$ unknowns - $\{x_i\}$, $\{y_i\}$ and pressure p . We use Gaussian elimination to solve for the $N_c + 2$ unknowns $\{\delta x_i\}$, δy_1 and δy_2 in terms of the remaining $N_c - 1$ unknowns $\delta y_3, \delta y_4, \dots, \delta y_{N_c}, \delta p$. Thus,

$$\begin{matrix} \delta x_1 \\ \delta x_2 \\ \vdots \\ \delta x_{N_c} \\ \delta y_1 \\ \delta y_2 \end{matrix} = \begin{pmatrix} a_{1,1} & a_{1,2} & \dots & a_{1,N_c-1} \\ a_{2,1} & a_{2,2} & \dots & a_{2,N_c-1} \\ \vdots & \vdots & \ddots & \vdots \\ a_{N_c+2,1} & \dots & \dots & a_{N_c+2,N_c-1} \end{pmatrix} \begin{matrix} \delta y_3 \\ \delta y_4 \\ \vdots \\ \delta y_{N_c} \\ \delta p \end{matrix} + \begin{matrix} b_1 \\ b_2 \\ \vdots \\ b_{N_c+2} \end{matrix} \quad (25)$$

The mass balance Equations (1) - (2), with terms expanded as described above, are $N_c + 1$ equations in the $2N_c + 4$ unknowns $\{\delta P_j\}$. Equation (25) is used to eliminate the $N_c + 2$ unknowns $\{\delta x_1, \delta x_2, \dots, \delta x_{N_c}, \delta y_1, \delta y_2\}$ and Equation (24) is used to eliminate δS_w . This elimination of $N_c + 3$ unknowns leaves a set of $N_c + 1$ primary

(mass balance) equations in $N_c + 1$ unknowns. This set of equations can be written in matrix form as

$$C \delta P = A(TA\delta P) + R \quad (26)$$

where C and T are $(N_c + 1) \times (N_c + 1)$ matrices, δP is the column vector $\{\delta y_3, \delta y_4, \dots, \delta y_{N_c}, \delta p, \delta S_o, \delta S_g\}$ and R is an $(N_c + 1) \times 1$ column vector consisting of residual terms dependent upon latest iterate values of fluid and rock properties. These primary equations are solved by the reduced band-width direct solution technique described by Price and Coats¹⁷.

After solution of Equation (26) for δP , the eliminated unknowns $\{\delta x_1, \delta x_2, \dots, \delta y_2\}$ are calculated from Equations (25) and δS_w is calculated from Equation (24). All $2N_c + 4$ unknowns are then updated as

$$P_{j,n+1} \approx P_j^{l+1} = P_j^l + \delta P_j \quad j=1,2,\dots,N \quad (27)$$

where a damping factor may be used on δP_j if iterate changes are excessive.

The values P_j^{l+1} are used to reevaluate terms in C , T , and R in Equation (26) and the latter equation is solved again. These iterations continue until $\max|\delta P_j|$ over the grid are less than specified tolerances. We generally use 1 psi for pressure, .01 for saturations and .002 for mol fractions.

Variable Substitution

The above description of the model formulation treats the general case where both oil and gas phases are present. If no free gas is present then the $2N_c + 4$ model equations (1) - (5) become $N_c + 3$ equations in the $N_c + 3$ unknowns $\{x_1\}$, p , S_o , S_w . The $N_c + 1$ deleted equations are the N_c fugacity constraints, Equations (3), and the gas phase mol fraction constraint, Equation (4b). The corresponding $N_c + 1$ deleted unknowns are $\{y_1\}$ and S_g .

The $N_c + 3$ equations are expanded as described above as linear combinations of the $N_c + 3$ variables $\{\delta P_j\} = \{\delta x_1, \delta x_2, \dots, \delta x_{N_c}, \delta p, \delta S_o, \delta S_w\}$. The set of $N_c + 1$ primary equations is obtained by eliminating δx_{N_c} using Equation (23a) and δS_w using Equation (24) with $\delta S_g = S_g^l = 0$. The remaining set of $N_c + 1$ primary variables is $\{\delta x_1, \delta x_2, \dots, \delta x_{N_c-1}, \delta p, \delta S_o\}$.

A similar variable substitution is performed for the case where oil saturation is zero. In any case, we always solve $N_c + 1$ simultaneous, primary equations in $N_c + 1$ unknowns by direct solution. In general, of course, adjacent grid blocks may have different sets of primary variables.

Case of Water Immobility

If water is present but immobile throughout the reservoir then the right-hand side of the water mass balance, Equation (2), is zero and that equation may be treated as a constraint equation as opposed to a primary equation. This reduction to N_c rather than $N_c + 1$ primary equations can be important since the computing time associated with direct solution of n simultaneous equations is proportional to n^3 ¹⁹.

If water is immobile then the model formulation is as described above with the following exception. The variable δS_w is eliminated from expanded Equation (2) and constraint Equation (24). The resulting equation in δS_o and δS_g is then used to eliminate δS_g from the N_c expanded component mass balance Equations (1). The resulting N_c primary variables then include only one saturation, δS_o , for the case where oil and gas phases are present and no saturations when oil or gas phase saturation is zero.

Hydrocarbon Phase Appearance/Disappearance

The case of hydrocarbon phase disappearance during a time step is quite simple. If both oil and gas phases are present in a grid block at the end of iteration l then the solution $\{P_j\}^{l+1}$ includes S_o^{l+1} and S_g^{l+1} . If either of these saturations is negative then it is set to zero before initiating the next iteration.

If S_o^l or S_g^l is zero in a grid block, then a saturation pressure calculation, described in the Appendix, is performed for the block's single-phase hydrocarbon fluid. If calculated p_g is less than the grid block pressure p^l then the block remains in single hydrocarbon phase mode. If p_g exceeds p^l then the absent phase saturation is set to (say) .001 and the present hydrocarbon phase S^l is decremented by .001. We apply this test each iteration. The saturation pressure calculation is not performed for two (hydrocarbon) phase grid blocks.

Numerical Dispersion Controls

As discussed under Applications below, multiple-contact-miscibility calculations exhibit considerable numerical dispersion. One occurrence of this numerical dispersion is at the leading edge of the two-phase (gas-

oil) displacement. The region downstream of this leading edge or gas saturation "shock" front should consist of oil at original composition*. With no control, the calculated oil composition is appreciably smeared downstream from this front. We effectively prevent this numerical dispersion by specifying oil outflow composition as original oil composition for each grid block until a gas phase appears in the block.

DISCUSSION OF MODEL FORMULATION

We summarize here some advantageous features of this formulation which are absent from some or all of the earlier reported models^{1-7,12}. The formulation is three-dimensional and treats flow of all three (gas, oil and water) phases accounting for capillary and gravity as well as viscous forces. Hydrocarbon phase relative permeability and capillary pressure are dependent upon interfacial tension in addition to saturation.

The implicit nature of the formulation removes a time step limitation associated with models using explicit transmissibilities. In the latter case, a single (hydrocarbon) phase grid block cannot experience a throughput (volumetric flow in or out) larger than the phase's volume in place in the block. In some cross-sections and/or single-well radial-z calculations, the corresponding time step limitation can be severe.

The "price" paid by the implicit formulation for this tolerance of larger time steps is the increased arithmetic per time step required for simultaneous solution of $N_c + 1$ primary equations. As the number of components becomes larger this penalty increases rapidly and must be offset by use of increasingly larger time steps than explicit formulations. The developing use of vector or array processor hardware may significantly reduce the ratio of equation-solution to coefficient-generation time with a result more favorable to implicit than explicit formulations.

The formulation described here does not generate or use equilibrium K-values per se and requires no flash calculation. However, the fugacity constraints are entirely equivalent to the direct use of K-values as $y_i = K_i x_i$ and one iteration of the flash calculation is automatically incorporated or performed in each overall iteration for each two-phase grid block.

Fussell and Fussell¹² report selection of two different reduced sets of equations and iteration variables for a two-phase grid block, depending upon whether the block is predominantly liquid or vapor. Our formulation uses a fixed set of reduced (primary) equations and variables for all saturations $0 < S < 1.0$.

*Physical dispersion or mechanical mixing will actually result in some smearing of oil composition at this front but the mixed zone is small compared with that produced by numerical dispersion.

The use of an equation of state, together with use of equation of state densities in the Lohrenz et al viscosity calculation¹⁵, ensures smooth convergence of phase compositions and all properties to critical point values as the latter is approached.

APPLICATIONS

In applications to date we have experienced little difficulty and few "surprises" in simulating depletion or cycling operations. However we have faced numerical dispersion and convergence problems in testing the model with the multiple-contact-miscibility type of problem. We are currently satisfied with the convergence attained by the implicit formulation described above but feel that numerical dispersion deserves further attention and attempts at control.

The applications described here include one- and two-dimensional (cross-sectional) example problems. Water is present but immobile in all calculations. The methane-butane-decane system is used for the reservoir hydrocarbon content. Reservoir temperature is 160°F for all calculations. Methane, butane and decane are referred to hereafter as components 1, 2 and 3, respectively.

As described in the Appendix, the modified Redlich-Kwong equation of state¹⁴ requires values for parameters Ω_{ai} , Ω_{bi} for each component and binary interaction coefficients C_{ij} . We calculated Ω_{ai} , Ω_{bi} at 160°F as described in the Appendix. Binary interaction coefficients $C_{ij} = 0$ except for $C_{12} = .024$, $C_{23} = .025$ were obtained from Zudkevitch and Joffe¹⁴.

Table 1 lists reported experimental data¹⁹ for the methane-butane-decane system and presents a comparison with our calculated saturation pressures and K-values using the above mentioned Ω_a , Ω_b , C_{ij} values. Zudkevitch and Joffe reported agreement between calculated and experimental results generally comparable with that shown in Table 1. However, their agreement was exact in regard to pressure and their calculated decane K-values were better at 160°F at 2000 and 3000 psia. Their unreported Ω_{ai} , Ω_{bi} values were undoubtedly somewhat different from ours as we use a somewhat different procedure to calculate them. However, Fussell and Fussell¹² imply their use of Zudkevitch and Joffe's procedure and the former give the Ω_{ai} , Ω_{bi} values at 160°F shown in Table 2. We used these values from Reference [12] and obtained no improvement in match of pressure or K-values.

The single-cell calculation described in the Appendix was used to calculate the critical point composition at 160°F and 2000 psia as $x_1 = .664$, $x_2 = .332$, $x_3 = .004$. The same calculation was used to determine a methane-butane composition necessary to generate multiple-contact-miscibility in a horizontal, one-dimensional displacement. An injected composition of $y_1 = .684$, $y_2 = .316$ was found to force the initial oil ($x_1 = .2$, $x_2 = .2$, $x_3 = .6$) exactly to the critical point. A leaner injection gas gave calculated oil disappearance with a disparity in phase compositions while a richer mixture gave either outright miscibility or a temporary gas phase which disappeared with disparity between phase compositions.

All fluid compositions mentioned here are mol fraction, not weight fraction.

One-Dimensional, Multiple-Contact-Miscibility Problem

Model Runs 1, 2 and 3 treat injection of a 68.4% methane - 31.6% butane gas mixture into a linear reservoir with 20% water saturation and 80% undersaturated oil saturation. Oil composition was 20% methane, 20% butane and 60% decane. Initial bubble point, reservoir temperature, and initial pressure were 821 psia, 160°F and 2000 psia, respectively. Initial oil in place, calculated by flashing the oil at stock tank conditions of 14.7 psia and 60°F, was 35,342 STB and stock tank gas-oil ratio was 267 SCF/STB.

The reservoir is 250 feet long, 100 feet wide and 50 feet thick. Permeability and porosity are 2000 md and .20, respectively. Other input data are listed in Table 3. 100 Mcf/day of gas were injected and production was on deliverability against a flowing bottomhole pressure of 2000 psia.

Runs 1, 2 and 3 were performed with specified, constant time steps of 1.875, 3.75 and 7.5 days, respectively, so that the ratio time step/cell volume was the same for all runs. The resulting maximum (over grid) changes in saturation and mol fraction per time step were generally each less than 0.1. However, at steps when phases converged to critical composition, saturation change per step was as high as 0.50.

Runs 1, 2 and 3 were performed using 80, 40 and 20 grid blocks, respectively. Figure 1 shows calculated gas saturation profiles vs distance at 210 days for the three runs. This figure shows a considerable effect of numerical dispersion on the rate of advance of the miscible front. The two-phase gas-oil zone saturations are less sensitive to number of grid blocks. Figure 2 further illustrates the increase in

calculated miscible front velocity with an increasing number of grid blocks.

Figure 3 shows calculated butane (intermediate component) mol fraction vs distance at 210 days. Initial butane mol fraction was .2 and injected butane mol fraction was .316. The calculations indicate an upstream miscible zone of injected gas composition, a two-phase zone of variable composition and a final, downstream single-phase oil zone of original oil composition. Actually, the downstream or leading portion of the two-phase zone should be a plateau of constant composition but its existence is masked by numerical dispersion effects. This plateau can be proven by the analytical solution technique of Welge et al²⁰ and is discussed by several authors^{6,7}. Figure 3 again shows that numerical dispersion is more pronounced in the vicinity of the miscible front than in the two-phase zone.

Figure 4 shows effect of grid block size on calculated oil rate and surface gas-oil ratio vs time. Finally, Figure 5 shows cumulative oil recovery vs time.

In all these runs, a given grid block progressed in time from original oil composition to a two-phase (gas-oil) configuration and finally to a single-phase (miscible) mode. The gas and oil phase compositions during the two-phase period continuously converged toward critical composition. The two-phase to single-phase transition occurred due to phase convergence - i.e. convergence of both phase compositions to critical composition - rather than oil or gas phase disappearance with a phase composition disparity.

Of the above discussed results, perhaps the least sensitive to effects of numerical dispersion is calculated cumulative oil recovery vs time. However, the 80-block Run 1 is not the "correct" answer in that it still displays numerical dispersion effects. Other authors presenting one-dimensional, multiple-contact-miscibility numerical calculations mention use of 100 and up to 300 grid blocks^{9,6}. Elimination or significant reduction of numerical dispersion in 10 - 20 grid block representations obviously requires control measures undiscovered in this study. Attempts to analyze and control this dispersion are discussed by several authors^{6,7,21}.

Welge et al²⁰ report that their analytical solution for this type of problem shows that saturation and composition profiles are unique but simply "stretch" with time. This implies that use of grid block size in-

creasing with distance from the injection well might reduce space truncation error using a fixed total number of cells. This idea was in effect used in an earlier study⁷ where grid block size was increased in groups from injector to producer. We repeated the 20-block Run 3 with $\Delta x_1 = \alpha \Delta x_{i-1}$ and $\alpha = 1.15$ so that Δx_1 was 2.44 feet and Δx_{20} was 34.73. Compared to the constant - Δx Run 3, agreement with the 80-block run was better at early time but worse at later time.

Two-Dimensional, Gas Injection Runs

Cross-sectional, x-z Runs 4 - 7 were performed for gas injection into a highly stratified reservoir. We examined the effect on calculated oil recovery of permeable zone ordering, k_v/k_H ratio and injection gas composition. The example reservoir is 400 feet long, 100 feet wide, 80 feet thick and is represented by a 20 x 4 grid. Permeability of the four layers varies from 20 md to 2500 md. Initial oil saturation, pressure and composition are identical to those used in the one-dimensional Runs 1 - 3. Model input data different from or additional to those given in Table 3 are given in Table 4. Initial oil in place was 95007 STB.

In Runs 4 - 6, injection gas of 68.4 mol % methane, 31.6 mol % butane was injected at 100 Mcf/Day into all four layers in proportion to layer permeability-thickness product. The production well was completed in all four layers and produced on deliverability against a 2000 psia flowing bottomhole pressure.

For Run 4, permeabilities were 20, 100, 500 and 2500 md in layers 1, 2, 3 and 4 (top to bottom), respectively and the k_v/k_H ratio was 1.0. The only change for Run 5 was reduction of k_v/k_H to 0.1. Run 6 had a k_v/k_H of 1.0 but the layer ordering was reversed with layer 1 - 4 permeabilities of 2500, 500, 100, and 20 md respectively.

Runs 4 - 7 were performed using automatic time steps controlled by maximum grid block changes (per time step, over entire grid) of .15 for both saturations and mol fractions.

The effect of the tenfold reduction in k_v/k_H was very little. The times of free gas appearance or breakthrough at the production well in layers 1 - 4 in Run 4 were 628, 900, 1020 and 1620 days, respectively. The corresponding times for Run 5 were 870, 745, 990 and 1350 days. Thus gas broke through most rapidly in layer 1 for Run 4 but in layer 2 for Run 5. In spite of the pronounced permeability increase with depth, Run 4 indicated a rather strong gas override. When free gas broke through in layer 1, the free gas fronts in layers 2, 3, and 4 were advanced only 65%, 55% and 15%, respectively, of the distance from injector to producer. In Runs 4 and 5, only a very limited miscible zone was present at 2160 days. This zone existed only in layer 3 a distance of about 30% of reservoir length from the injector.

Figure 6 compares calculated oil recovery and GOR vs time for Runs 4 and 6. In Run 6, free gas broke through at the producer in layer 1 at 262 days and in layer 2 at 1338 days. The high permeability at formation top in Run 6 aggravated the gas override and reduced oil recovery from over 90% to 53% of original oil in place. In run 6 the miscible zone existed only in layer 1 and broke through at the producer at 1570 days. While this miscible zone initially appeared with phase convergence at critical composition, the gas composition subsequently became leaner than the injected composition due to percolation or upward flow from layer 2 of leaner, immiscible (in layer 2) gas. The calculated methane mol fraction of layer 1 gas was uniformly 70% at 2160 days.

Run 7 is the same as Run 4, with the permeable layer at the bottom and $k_v/k_H = 1$, but injection gas is a lean 90 mol % methane, 10 mol % butane. Figure 7 shows that the lean gas injection gives somewhat higher early oil recovery but gas overrides and breaks through quickly at 379 days in layer 1 and 394 days in layer 2. Calculated GOR rises rapidly and final recovery at 2160 days is only 59% of original oil in place, compared to 91% recovery for Run 4 using richer gas injection.

This lean gas of Run 7 is very similar to an equilibrium gas in that its composition lies very close to the phase envelope. Thus there is not a pronounced vaporization or condensation mechanism and no calculated oil saturation anywhere in the reservoir is reduced below .18. This "immiscible" character of the injected gas explains the early higher oil recovery (than Run 4) which is directly caused by slightly higher reservoir pressurization early in Run 7.

EFFICIENCY OF THE FORMULATION

Computing time requirement for a formulation is of interest since comparison of different formulations' overall efficiencies is helpful in continuing development efforts. All computing times mentioned here are CDC 6600 CPU seconds. One-dimensional Runs 1, 2 and 3 required .036 seconds per block-step for total run times of 872, 239 and 75 seconds, respectively. Average iterations per time step for each run were about 3.25.

Two-dimensional Runs 4 - 7 all were carried out to 2160 days. Run 4 required the most computing time, 474 seconds for 114 steps and 465 iterations, or an average of 4.08 iterations per time step. Computing time per block-step was .052 seconds.

Fussell and Fussell¹² reported a computing time requirement of .0066 - .0254 (CDC 6600) seconds per block-step for a 3-component problem for their semi-implicit equation of state compositional model. They actually reported IBM 370/168 times and we use a factor of 2.2 for CDC 6600 time/IBM 370/168 time. They reported calculated results for immiscible gas injection in a 13x9 cross-section, using the methane-butane-decane system, but did not give time step or overall computing time information.

We performed an 11x9 cross-sectional run similar to their example to determine the increased computing time requirement of this formulation due to an increase in band-width from 4 (in Runs 4 - 7) to 9. The computing time per block per iteration increased only from .0128 to .0159 seconds. The 1080 day run required 14 time steps, 115 seconds, and corresponds to .375 hydrocarbon pore volumes injected.

S. MARY

An implicit formulation utilizing an equation of state has been described for simulation of multidimensional, compositional problems. Applicability of the formulation ranges from cycling or depletion of volatile oil and gas condensate reservoirs to outright or multiple-contact miscible flooding operations.

Computational testing with example problems indicates stable convergence of this formulation as hydrocarbon phase compositions and properties converge near a critical point. Continuing effort is directed toward comparison of model results with laboratory results for both multiple-contact-miscibility and outright miscible cases.

The reported computational testing centered on the multiple-contact-miscibility process since ability to stably and efficiently compute behavior very close to a critical point is perhaps the severest test of a compositional formulation. Our example problem results for this process indicate significant numerical dispersion primarily affecting the calculated velocity of miscible-front advance. Further effort is required to analyze and reduce this numerical dispersion.

While we report detailed problem descriptions, results and associated computing times, we lack similar reported times necessary to assess the relative overall efficiency of an implicit formulation as opposed to semi-implicit formulations.

NOMENCLATURE

c_r	Rock compressibility, 1/psi
c_w	Water compressibility, 1/psi
C_{ij}	Modified Redlich-Kwong equation binary interaction coefficients
f	Fugacity, psia
f_i	Fugacity of component i in a mixture
k_v	Vertical permeability
k_H	Horizontal permeability
k	Permeability, md x.00633
k_r	Relative permeability, fraction
k_{rgcw}	Relative permeability to gas at connate water
k_{rocw}	Relative permeability to oil at connate water

K_i	Equilibrium K-value for component i , y_i/x_i
N_c	Number of hydrocarbon components
N	$2N_c + 4$
n_w, n_{ow}, n_{og}	Exponents on relative permeability curves
n_g	
P_{chi}	Parachor of component i
PI_k	Layer k productivity index, cu.ft. - cp/day-psi
P_i	Unknowns, see Equation (6)
P_{cgo}	Gas-oil capillary pressure, $p_g - p_o$, psi
P_{cwo}	Water-oil capillary pressure, $p_o - p_w$, psi
P_s	Saturation Pressure
P_o	Original reservoir pressure
P	Gas phase pressure, psia
q_i	Production rate of component i from grid block, mols/day
q_w	Water production rate, mols/day
R	Universal gas constant, 1.98 Btu/lb mol - °R
S	Phase saturation, fraction
S_{gc}	Critical gas saturation
S_{org}	Residual oil saturation to gas
S_{orw}	Residual oil saturation to water
S_{gr}	Residual gas saturation
S_{wir}	Irreducible water saturation
T	Temperature, °R
t	Time, days
Δt	Time step, days
\underline{V}	Specific volume, cu.ft./lb mol
V	Grid block volume, $\Delta x \Delta y \Delta z$
$\Delta x, \Delta y, \Delta z$	Grid block dimensions, feet
x_i	Mol fraction of component i in oil phase
y_i	Mol fraction of component i in gas phase
Z	Subsea depth, measured positively downward, feet
Z_k	Depth to center of layer k

Greek

γ	Specific weight, psi/ft
λ	Phase mobility, k_r/μ
ψ_1	Fugacity coefficient of component 1, $f_1/p x_1$
ρ	Density, mols/cu.ft.
ϕ	Porosity, fraction, $\phi_0(1 + c_r(p - p_0))$
ω	Acentric factor
σ	Interfacial tension, dynes/cm.
Ω_a, Ω_b	Redlich-Kwong equation parameters
T	Fluid flow transmissibility, kA/L , reservoir cu.ft-cp/day-psi
μ	Viscosity, cp

Difference Notation

X is any quantity or arithmetic expression

$\Delta X = X_1 - X_2$ where subscripts 1 and 2 refer to adjacent grid blocks "1" and "2"

$$\Delta(T\Delta X) \equiv \Delta_x(T_x \Delta_x X) + \Delta_y(T_y \Delta_y X) + \Delta_z(T_z \Delta_z X)$$

$$\Delta_x(T_x \Delta_x X) \equiv T_{x,i+\frac{1}{2}}(X_{i+1} - X_i) - T_{x,i-\frac{1}{2}}(X_i - X_{i-1})$$

where $T_{x,i+\frac{1}{2}}$ is x -direction transmissibility for flow between grid blocks i and $i+1$ and X_i is the value of X at grid block i . Subscripts j and k are suppressed here.

Subscripts

c	Critical
g	Gas
h	Heavy hydrocarbon component
i	Component
i, j, k	Grid block indices in x, y and z directions
L	Hydrocarbon liquid phase
n	Time step level
o	Oil
s	Saturated condition
w	Water
wb	Wellbore

V	Gas phase
$1, 2$	Adjacent grid blocks 1 and 2

Superscripts

o	Original
l	Iteration number
L	Hydrocarbon liquid phase
V	Hydrocarbon gas phase

REFERENCES

- Price, H.S., and Donohue, D.A.T.: "Isothermal Displacement Processes with Interphase Mass Transfer", Soc. Pet. Eng. J. (June, 1967), 205-220.
- Roebuck, I.F., Jr., Henderson, G.E., Douglas, Jim Jr., and Ford, W.T.: "The Compositional Reservoir Simulator: Case 1--The Linear Model", Soc. Pet. Eng. J. (March, 1969) 115-130.
- Culham, W.E., Farouq Ali, S.M., and Stahl, C.D.: "Experimental and Numerical Simulation of Two-Phase Flow with Interphase Mass Transfer in One and Two Dimensions", Soc. Pet. Eng. J. (September, 1969) 323-337.
- Kniazeff, V.J., and Naville, S.A.: "Two-Phase Flow of Volatile Hydrocarbons", Soc. Pet. Eng. J. (March, 1965) 37-44; Trans., AIME 234.
- Nolen, J.S.: "Numerical Simulation of Compositional Phenomena in Petroleum Reservoirs", SPE Reprint Series No. 11, Numerical Simulation (1073) 269-284.
- Van Quy, N., Simandoux, P., and Corteville, J.: "A Numerical Study of Diphasic Multicomponent Flow", Soc. Pet. Eng. J. (April, 1972) 171-184; Trans., AIME, Vol. 253.
- Corteville, J., Van Quy, N., and Simandoux, P.: "A Numerical and Experimental Study of Miscible or Immiscible Fluid Flow in Porous Media with Interphase Mass Transfer", paper SPE 3481 presented at SPE-AIME 46th Annual Fall Meeting, New Orleans.
- Metcalf, R.S., Fussell, D.D., and Shelton, J.L.: "A Multicell Equilibrium Separation Model for the Study of Multiple Contact Miscibility in Rich-Gas Drives", Soc. Pet. Eng. J. (June, 1973) 147-155.
- Fussell, D.D., Shelton, J.L., and Griffith, J.D.: "Effect of 'Rich' Gas Composition on Multiple-Contact Miscible Displacement--A Cell-to-Cell Flash Model Study", Soc. Pet. Eng. J. (December, 1976) 310-316.
- Cook, Alton B., Walter, C.J., and Spencer, George C.: "Realistic K-Values of C_7+ Hydrocarbons for Calculating Oil Vaporization During Gas Cycling at High Pressure", J. Pet. Tech. (July, 1969) 901-915; Trans., AIME, Vol. 246.

11. Fussell, D.D., and Yanosik, J.L.: "An Iterative Sequence for Phase Equilibria Calculations Incorporating the Redlich-Kwong Equation of State", Soc. Pet. Eng. J. (June, 1978) 173-182.
12. Fussell, L.T., and Fussell, D.D.: "An Iterative Sequence for Compositional Reservoir Models Incorporating the Redlich-Kwong Equation of State", paper SPE 6891 presented at the SPE-AIME 52nd Annual Fall Meeting, Denver, Colorado (October 9-12, 1977).
13. Redlich, O., and Kwong, J.N.S.: Chem. Rev. 44 (1949) 233.
14. Zudkevitch, David, and Joffe, Joseph: "Correlation and Prediction of Vapor-Liquid Equilibria with the Redlich-Kwong Equation of State", AIChE Journal (January, 1970) Vol. 16, No. 1, 2-119.
15. Lohrenz, J., Bray, B.G., and Clark, C.R.: "Calculating Viscosity of Reservoir Fluids from Their Composition", J. Pet. Tech. (October, 1964) 1171-1176; Trans., AIME, Vol. 231.
16. Reid, R.C., and Sherwood, T.K.: The Properties of Gases and Liquids, 3rd Edition, McGraw-Hill Book Co., Inc., New York (1977).
17. Price, H.S., and Coats, K.H.: "Direct Methods in Reservoir Simulation", Soc. Pet. Eng. J. (June, 1974) 295-308; Trans., AIME, Vol. 257.
18. Coats, K.H.: "A Highly Implicit Steamflood Model", Soc. Pet. Eng. J. (October, 1978) 369-383.
19. Reamer, H.H., Fiskin, J.M., and Sage, B.H.: Ind. Eng. Chem., 41, 2871-5 (1949).
20. Welge, H.J., Johnson, E.F., Ewing, S.P., and Brinkman, F.H.: J. Pet. Tech. (August, 1961) 787-96.
21. Camy, J.P., and Emanuel, A.S.: "Effect of Grid Size in the Compositional Simulation of CO₂ Injection", paper SPE 6894 presented at the SPE-AIME, 52nd Annual Fall Meeting, Denver, Colorado (October 9-12, 1977).
22. Yarborough, L.: "Application of a Generalized Equation of State to Petroleum Reservoir Fluids", paper presented at the Symposium of Equations of State in Engineering and Research at the 176th ACS National Meeting, Miami Beach, Florida (September 10-15, 1978).
23. Coats, K.H.: "In-Situ Combustion Model", paper SPE 8394 presented at the SPE-AIME 54th Annual Fall Technical Conference and Exhibition, Las Vegas, Nevada (September 23-26, 1979).
24. Stone, H.L.: "Estimation of Three-Phase Relative Permeability and Residual Oil Data", J. Can. Pet. Tech. (October-December, 1973) 53-61.
25. Peng, D.Y., and Robinson, D.B.: "A Rigorous Method for Predicting the Critical Properties of Multicomponent Systems from an Equation of State", AIChE J. 23, 137-144 (1977).
26. Baker, Lee E., and Kraemer, P.L.: "Critical Point and Saturation Pressure Calculations for Multicomponent Systems", paper SPE 7478 presented at the SPE-AIME 53rd Annual Fall Meeting, Houston, Texas (October 1-3, 1978).

APPENDIX

PVT TREATMENT

Hydrocarbon liquid and gas phase densities and component fugacities are computed from the Redlich-Kwong equation of state¹³ in a modified form nearly identical to that described by Zudkevitch and Joffe¹⁴. A recent paper by Yarborough²² discusses this modified equation and presents detailed results of its application to reservoir fluids. In part, he provides a number of binary interaction coefficients for this equation of interest in reservoir work.

The modified equation is

$$P = \frac{RT}{V-b} - \frac{a}{T^{1.5}V(V+b)} \quad (30)$$

where for a liquid phase mixture,

$$a = \sum_{i=1}^N \sum_{j=1}^N x_i x_j a_{ij} \quad (31)$$

$$a_{ij} = (1 - C_{ij})(a_i a_j)^{.5} \quad (32)$$

$$a_i = \Omega_{ai} R^2 T_{ci}^{2.5} / p_{ci} \quad (33)$$

$$b = \sum x_i b_i \quad (34)$$

$$b_i = \Omega_{bi} R T_{ci} / p_{ci} \quad (35)$$

$$C_{ij} = \text{binary interaction coefficient.}$$

For a gas phase mixture, y_i are used in place of x_i in Equations (31) and (34). Equation (30) can be written in terms of compressibility factor as

$$z^3 - z^2 + (A - B^2 - B)z - AB = 0 \quad (36)$$

where

$$A = ap/R^2 T^{2.5} \quad (37)$$

$$B = bp/RT \quad (38)$$

The fugacity coefficient of component i in a mixture is $\psi_i \equiv f_i/p_{x_i}$ and is defined by¹⁶

$$RT \ln \psi_i = - \int_{\infty}^V \left(\frac{\partial p}{\partial N_i} - \frac{RT}{V} \right) dV - RT \ln z \quad (39)$$

where V here is total volume of N mixture moles and N_i is moles of component i in the mixture.

Using Equation (30) in (39) gives

$$\frac{f_i}{p x_i} = \psi_i = \frac{1}{z-B} \left(\frac{z+B}{B} \right)^{E_i} e^{\frac{B_i}{B}(z-1)} \quad (40)$$

where

$$E_i = \frac{A}{B} \left(\frac{B_i}{B} - \frac{2}{A} \sum_{j=1}^N x_j A_{ij} \right) \quad (41)$$

$$A_{ij} = a_{ij} p / R T^{2.5} \quad (42)$$

$$B_i = b_i p / RT \quad (43)$$

The expression (40) for component fugacity is derived or given by a number of authors¹¹⁻¹⁴.

Equations (36) and (40) apply separately to the liquid and gas hydrocarbon phases with mole fractions $\{x_i\}$ and $\{y_i\}$ used, respectively, in calculating A , B and other composition-dependent terms. In Equation (40), z_L or z_G is used when the equation is applied to the liquid or gas phase, respectively.

For the unmodified Redlich-Kwong equation¹³, $\Omega_a = .4274802327$, $\Omega_b = .08664035$ and are independent of temperature, pressure, composition and particular component. Zudkevitch and Joffe¹⁴ calculate Ω_{ai} , Ω_{bi} for each component i at a given temperature utilizing the component's saturation pressure, saturated liquid density and Lyckman's fugacity coefficient.

We calculate Ω_{ai} and Ω_{bi} at any temperature from the two equations

$$f_i^L = f_i^V \quad (44)$$

$$z_i^L = z_{ci} \quad (45)$$

where z_{ci} is critical z -factor of the component and pressure is specified as the saturation pressure at the given temperature. Equations (44) and (45) are therefore two equations in the two unknowns Ω_{ai} , Ω_{bi} and are solved using the Newton-Raphson method.

Results described in this paper were obtained using Reidel's vapor-pressure equation¹⁶ and Gunn and Yamada's method¹⁶ to obtain saturated pressures and liquid densities.

If the temperature T is above T_c for the component, then we utilize critical properties to determine Ω_{ai} , Ω_{bi} as suggested by Zudkevitch and Joffe. We use z_{ci} and their suggested critical fugacity

$$\ln \psi_{ci} = -.1754 - .0361 \omega_i \quad (46)$$

where ω is component i acentric factor. Thus the two equations for determining Ω_{ai} , Ω_{bi} for $T > T_c$ are

$$\psi^L(A, B) - \psi_{ci} = 0 \quad (47a)$$

$$z(A, B) - z_{ci} = 0 \quad (47b)$$

with $T = T_c$, $p = p_c$.

Phase Density Calculation

Hydrocarbon liquid and gas phase densities are calculated as

$$\rho = p / zRT \quad (48)$$

where z is obtained from the latest iterate phase composition and pressure values by solution of Equation (36) using the analytical solution for a cubic equation. Derivatives of ρ_0 with respect to $\{x_i\}$ and pressure are obtained as

$$\frac{\partial \rho_0}{\partial p} = \left(1 - \frac{1}{z_L} \frac{\partial z_L}{\partial p} \right) / z_L RT \quad (49)$$

$$\frac{\partial \rho_0}{\partial x_i} = - \frac{p}{z_L^2 RT} \frac{\partial z_L}{\partial x_i} \quad (50)$$

where Equation (36) gives

$$\frac{\partial z_L}{\partial p} = \frac{\partial z_L}{\partial A} \frac{\partial A}{\partial p} + \frac{\partial z_L}{\partial B} \frac{\partial B}{\partial p} \quad (51)$$

$$\frac{\partial z_L}{\partial x_i} = \frac{\partial z_L}{\partial A} \frac{\partial A}{\partial x_i} + \frac{\partial z_L}{\partial B} \frac{\partial B}{\partial x_i} \quad (52)$$

and

$$\frac{\partial z_L}{\partial A} = (B - z_L) / (3z_L^2 - 2z_L + A - B^2 - B) \quad (53)$$

$$\frac{\partial z_L}{\partial B} = (A + (2B + 1)z_L) / (3z_L^2 - 2z_L + A - B^2 - B) \quad (54)$$

The derivatives $\partial A / \partial p$, $\partial A / \partial x_i$, etc., are calculated from Equations (37), (38) and (31)-(35). Calculation of gas phase density derivatives is identical except that z_v and $\{y_i\}$ replace z_L and $\{x_i\}$.

Saturation Pressure Calculation

Saturation pressure is calculated in the manner proposed by Fussell and Yanosik¹¹ with one minor exception. They propose solution of the $N_c + 1$ equations

$$f_i^L - f_i^V = 0 \quad i=1, 2, \dots, N_c \quad (55)$$

$$P_s - \sum_{j=1}^{N_c} \frac{f_j^L}{\psi_j^V} = 0 \quad (56)$$

for the $N_c + 1$ unknowns $\{y_1, y_2, \dots, y_{N_c}, p_g\}$ using the Newton-Raphson method to obtain saturation pressure of a liquid phase. We have found somewhat improved convergence by replacing Equation (56) by

$$\sum_{j=1}^{N_c} y_j = 1.0 \quad (57)$$

This saturation pressure calculation is performed each iteration for each grid block where $S_g = 0$ or $S_o = 0$. The recalculated saturation pressure and absent phase composition are stored and used as starting values for the next iteration's Newton-Raphson solution of Equations (55) and (57).

Fugacity Calculation

Hydrocarbon liquid and gas phase component fugacities and their derivatives are calculated each iteration for all three-phase (including water) grid blocks from Equations (40) and (36) using latest iterate values of composition and pressure. The phase z-factor is first calculated from Equation (36) along with derivatives of z with respect to composition and pressure.

Relative Permeability

Analytical representations for individual phase relative permeabilities are used here in describing the relative permeability calculations. The model has the option of reading tabular data in lieu of the analytical forms. k_{rw} and k_{row} denote relative permeabilities to water and oil, respectively, measured in a core containing no free gas. k_{rog} and k_{rg} are relative permeabilities to oil and gas measured in the core containing irreducible water saturation.

Under immiscible conditions, gas-oil relative permeability curves generally exhibit considerable curvature and residual gas and residual oil saturations below which the respective phases are immobile. Near a critical point, however, interfacial tension approaches zero, residual phase saturations decrease toward zero and the relative permeability curves must approach straight lines. The treatment given here is not based on any theory or experimental evidence; it is simply devised to exhibit the described behavior with interfacial tension reduction.

The two-phase gas and oil curves used in this work are

$$k_{rg} = k_{rgcw} [f(\sigma) \bar{S}_g^n + (1 - f(\sigma)) \bar{S}_g] \quad (58)$$

$$k_{rog} = f(\sigma) \bar{S}_o^n + (1 - f(\sigma)) \bar{S}_o \quad (59)$$

where

$$\bar{S}_g = \frac{S_g - S_{gr}^*}{1 - S_{wir} - S_{gr}^*} \quad (60)$$

$$\bar{S}_o = \frac{1 - S_g - S_{wir} - S_{org}^*}{1 - S_{wir} - S_{org}^*} \quad (61)$$

and

$$f(\sigma) = \left(\frac{\sigma}{\sigma_0}\right)^{n_1} \quad (62)$$

σ is interfacial tension, σ_0 is "initial" tension corresponding to the read-in capillary pressure curve and n_1 is a read-in exponent generally in the range of 4-10. $n_g, n_{og}, k_{rgcw}, k_{row}, S_{wir}, S_{org},$ and S_{gr} are input data. As interfacial tension decreases, S_{gr}^* and S_{org}^* approach zero as

$$S_{gr}^* = f(\sigma) S_{gr} \quad (63)$$

$$S_{org}^* = f(\sigma) S_{org} \quad (64)$$

Gas phase relative permeability is treated with hysteresis as described elsewhere²³. Thus S_{gr}^* is also a function of S_{gmax} and S_g when S_g is less than S_{gmax} , where S_{gmax} is historical maximum gas saturation in the grid block.

For large n_1 , as σ decreases below σ_0 the value of $f(\sigma)$ will remain near 1.0 until σ/σ_0 is very small. This means that k_{rg} and k_{rog} given by Equations (58) and (59) will vary little with interfacial tension until close proximity to the critical point is attained. This reflects our understanding of the literature on low tension behavior which indicates that very low interfacial tensions are necessary to appreciably reduce residual oil saturations under normal reservoir pressure gradients.

In summary, Equations (58) - (64) give k_{rg} and k_{rog} of specified curvature with specified residual saturations S_{gr} and S_{org} at original gas-oil interfacial tension. As tension decreases toward zero the curves continuously approach straight lines with zero residual saturations.

If water is immobile then $k_{rw} = 0$ and $k_{ro} = k_{row} \times k_{rog}$ as described above. For the three-phase case,

$$k_{ro} = k_{row} [(k_{row} + k_{rw})(k_{rog} + k_{rg}) - k_{rw} - k_{ro}] \quad (65)$$

which is Stone's method²⁴ modified slightly for the case where k_{row} is less than 1. Analytical relationships used for k_{rw} and k_{row} are

$$k_{rw} = k_{rwro} \left(\frac{S_w - S_{wir}}{1 - S_{wir} - S_{orw}} \right)^{n_w} \quad (66)$$

$$k_{row} = \left(\frac{1 - S_w - S_{orw}}{1 - S_{wir} - S_{orw}} \right)^{n_{ow}} \quad (67)$$

Interfacial Tension and Capillary Pressure

The gas-oil interfacial tension is calculated from the Macleod - Sugden correlation¹⁶

$$\sigma^{\frac{1}{2}} = \sum_{i=1}^{N_c} P_{chi} (\rho_L x_i - \rho_g y_i) \quad (68)$$

where P_{chi} is the parachor of component i and densities (here only) are in units of $g\text{-mol}/cm^3$. If a gas cap is initially present in the reservoir the σ_0 is calculated from Equation (68) using the equilibrium phase densities and compositions. If the original reservoir oil is undersaturated then saturation pressure (bubble point) is calculated and σ_0 is calculated from Equation (68) using equilibrium phase densities and compositions at that pressure.

The read-in gas-oil capillary pressure curve is assumed to correspond to a tension of σ_0 . At any other interfacial tension, the read-in P_{cgo} is multiplied by σ/σ_0 . Input capillary pressures can be expressed in tabular or analytical form. In this work we used analytical expressions

$$P_{cwo} = a_w + b_w (1 - S_w) + c_w (1 - S_w)^3 \quad (69)$$

$$P_{cgo} = a_g + b_g S_g + c_g S_g^3 \quad (70)$$

Viscosity Treatment

Water viscosity is a constant read as input data. Gas and oil phase viscosities are computed using the Lohrenz, Bray and Clark method¹⁵. The phase densities in their method are obtained from the equation of state so that gas and oil phase viscosities converge to a common value as phase compositions converge near a critical point.

Calculation of Critical Composition

The model formulation described in the body of this paper has been programmed in single-cell or zero-dimensional material balance mode. Two recent papers^{25, 26} discuss a rigorous method of critical pressure, temperature and composition calculations. We have found that our problem is generally determination of critical composition at given pressure and temperature. We use this single-cell calculation for this

purpose. A critical point is determined for a specified initial oil composition, specified pressure and temperature and an injection gas composition having one degree of freedom. A series of gas injection runs are performed with the compositional "degree of freedom" varied. Each run simulates continued mixing of injected gas with the mixture resulting from gas and oil removal at constant pressure using relative permeability curves. By these trial and error runs, an injection composition is found which results in the cell's gas and oil phases converging at the critical composition. If injection gas is too lean then oil will disappear in the cell, or if too rich then gas will disappear, in either case with a significant disparity between final equilibrium gas and oil phase compositions. This single-cell type of calculation is discussed in detail in the literature⁸⁻¹⁰. We simply point out here that we have found it provides a rather quick and reliable procedure for calculating a critical composition. In addition, of course, the calculation gives a close estimate (in our experience) of the "minimum enrichment" injection composition necessary to achieve multiple-contact-miscibility. Fussell et al⁹ discuss this in greater detail and point out that the shape of relative permeability curves used in this calculation can affect the accuracy of this indicated minimum enrichment.

TABLE 1
COMPARISON OF CALCULATED AND EXPERIMENTAL
RESULTS FOR THE METHANE-BUTANE-DECANE SYSTEM¹⁹

<u>T, °F</u>	<u>x₁</u>	<u>p, psia</u>	<u>p, calculated</u>	<u>K-VALUE</u>	
				<u>Exp.</u> ¹⁹	<u>Calc.</u>
280	x ₁ =.203	1000	1019.7	K ₁ =3.813	3.773
	x ₂ =.346			K ₂ = .613	.637
	x ₃ =.451			K ₃ = .032	.031
280	.402	2000	1970.5	1.861	1.867
	.370			.605	.613
	.228			.122	.099
280	.575	3000	2997.6	1.459	1.475
	.179			.631	.635
	.246			.193	.156
160	.253	1000	972.7	3.174	3.173
	.661			.297	.297
	.086			.013	.008
160	.459	2000	1950.9	1.854	1.862
	.390			.367	.361
	.151			.039	.028
160	.663	3000	3128.2	1.213	1.254
	.229			.703	.633
	.108			.330	.218

TABLE 2
COMPARISON OF CALCULATED Ω_a , Ω_b VALUES
FOR METHANE, BUTANE AND DECANE

<u>Component</u>	<u>Ω_{ai}</u>		<u>Ω_{bi}</u>	
	<u>Ref. 12</u>	<u>This Work</u>	<u>Ref. 12</u>	<u>This Work</u>
methane	.4251	.42617	.0859	.086173
butane	.4154	.419367	.0759	.0794
decane	.46512	.451875	.07259	.070452

TABLE 3
MODEL DATA FOR RUNS 1-3

Reservoir length	250 ft.
Width	100 ft.
Thickness	50 ft.
Permeability	2000 md
Porosity	.2
$c_w = .000003$	
$c_r = .000004$	
One-dimensional grid	80 blocks, 40 blocks, 20 blocks (Runs 1, 2, 3)
Capillary pressure	zero
Relative permeability data:	
S_{wc}	.2
S_{org}	.2
S_{gc}	0
S_{gr}	.15
k_{rocw}	1.0
k_{rgcw}	1.0
k_{rw}	0
$n_{og} = n_g =$	2 (see Equations (58), (59))
Initial pressure	2000 psia
Reservoir temperature	160°F
Initial saturations:	
S_w, S_o, S_g	.2, .8, 0
Initial oil composition:	
x_1, x_2, x_3	.2, .2, .6
Initial calculated oil viscosity ¹⁵	1.07 cp
Stock tank conditions	14.7 psia, 60°F
100 Mcf/day of 68.4 mol% methane, 31.6 mol% butane injected at $x=0$	
Production at $x=250$ ft. on deliverability at 2000 psia	

TABLE 4

MODEL DATA FOR TWO-DIMENSIONAL RUNS 4-7

Reservoir length		400 ft.		
width		100 ft.		
	<u>Layer</u>	<u>k, md</u>	<u>φ</u>	<u>PI, RB-cp/day-psi</u>
	1	20	.18	2
	2	100	.20	10
	3	500	.22	50
	4	2500	.24	250

Layers were reversed in order for Run 6

$k_v/k_H = 1.0$ except for 0.1 value used in Run 5

Vertical permeability is calculated as harmonic average of adjacent layer permeabilities

$$P_{cgo} = 20 S_g^3$$

Injection = 100 Mcf/day of 68.4% methane, 31.6% butane, Runs 4-6
= 100 Mcf/day of 90% methane, 10% butane, Run 7

Production at $x=400$ ft. from all four layers on deliverability at 2000 psia opposite center of top layer

FIGURE 1
CALCULATED GAS SATURATION VS. DISTANCE

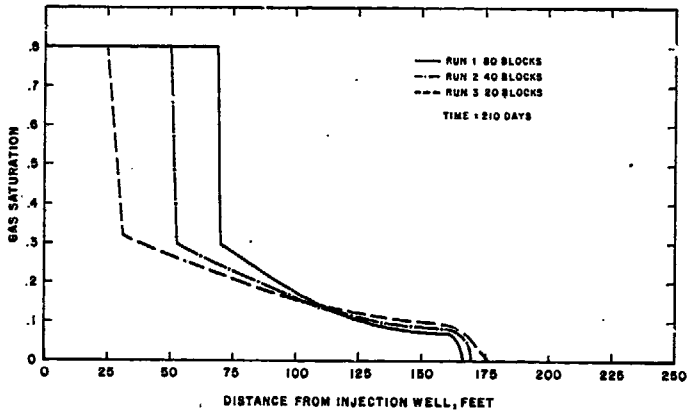


FIGURE 2
CALCULATED MISCIBLE FRONT ADVANCE VS. TIME

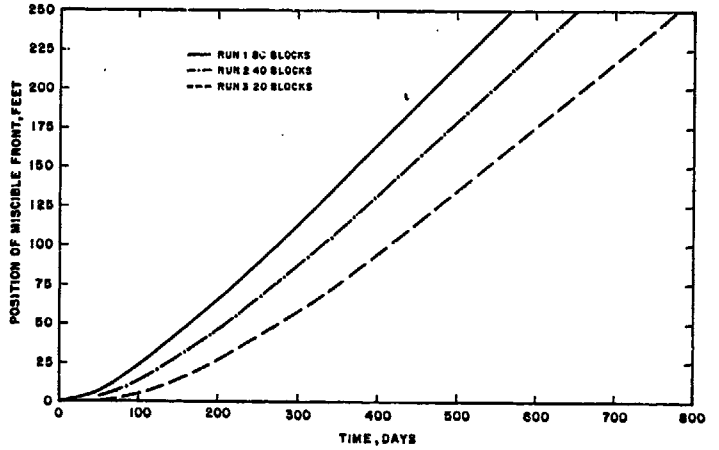


FIGURE 3
CALCULATED BUTANE MOL FRACTION VS. DISTANCE

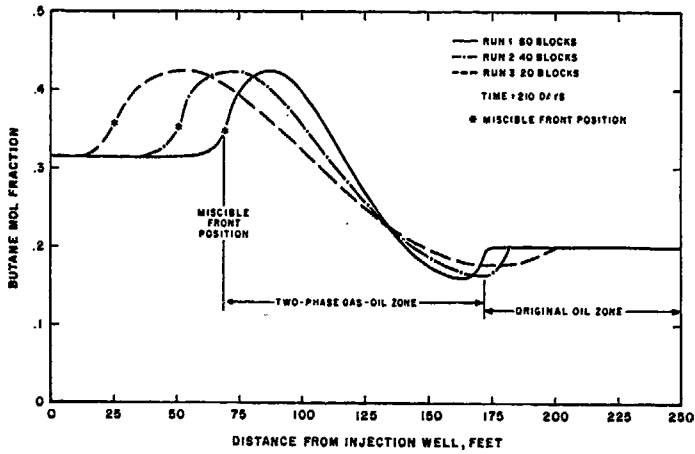
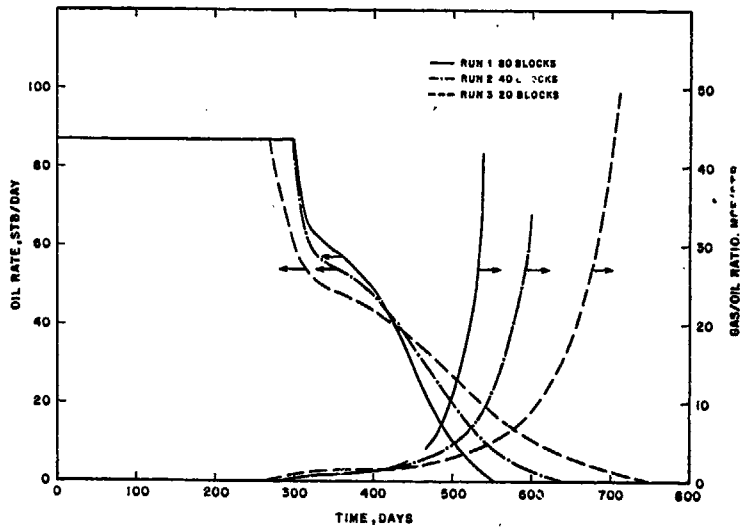
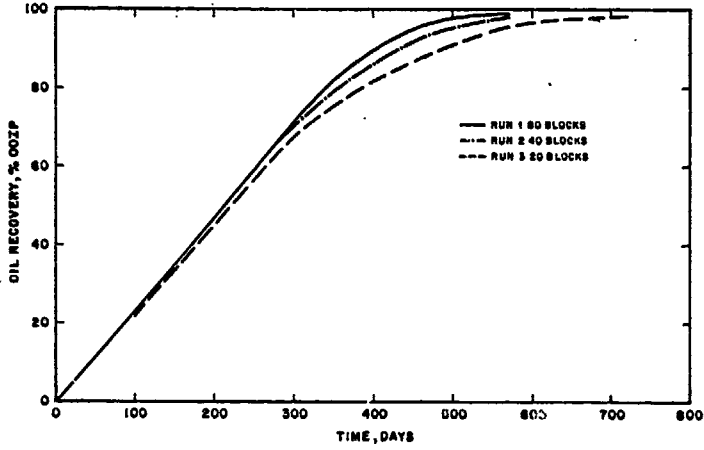


FIGURE 4
CALCULATED OIL PRODUCTION RATE AND GOR VS. TIME



**FIGURE 5
CALCULATED OIL RECOVERY VS. TIME**



**FIGURE 6
CALCULATED OIL RECOVERY AND GAS/OIL RATIO**

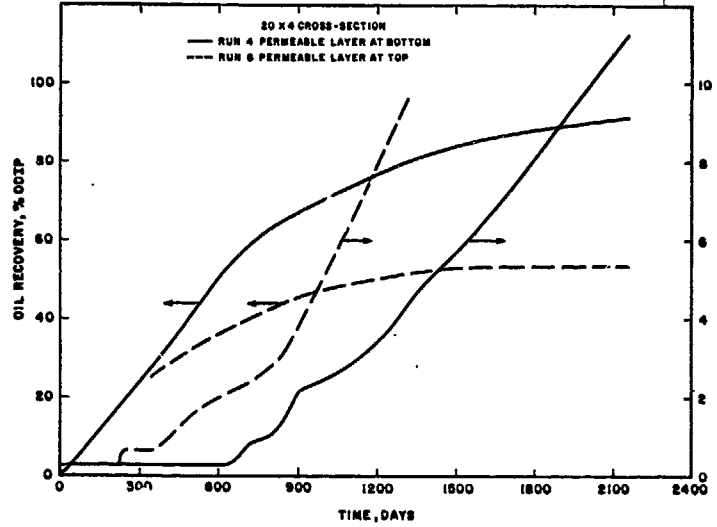


**FIGURE 7
CALCULATED OIL RECOVERY AND GAS/OIL RATIO**

